



HAL
open science

**Sensitivity to electron-to-proton mass ratio variation
from 12 C₂H₂ rovibrational transitions to $\nu_1 + \nu_3$ and
 $\nu_1 + \nu_2 + \nu_4 + \nu_5$ interacting levels**

Florin Lucian Constantin

► **To cite this version:**

Florin Lucian Constantin. Sensitivity to electron-to-proton mass ratio variation from 12 C₂H₂ rovibrational transitions to $\nu_1 + \nu_3$ and $\nu_1 + \nu_2 + \nu_4 + \nu_5$ interacting levels. *Vibrational Spectroscopy*, 2016, 85, pp.228-234. 10.1016/j.vibspec.2016.04.012 . hal-03335700

HAL Id: hal-03335700

<https://hal.science/hal-03335700v1>

Submitted on 23 Sep 2021

HAL is a multi-disciplinary open access archive for the deposit and dissemination of scientific research documents, whether they are published or not. The documents may come from teaching and research institutions in France or abroad, or from public or private research centers.

L'archive ouverte pluridisciplinaire **HAL**, est destinée au dépôt et à la diffusion de documents scientifiques de niveau recherche, publiés ou non, émanant des établissements d'enseignement et de recherche français ou étrangers, des laboratoires publics ou privés.

Sensitivity to electron-to-proton mass ratio variation from $^{12}\text{C}_2\text{H}_2$ rovibrational transitions to $\nu_1 + \nu_3$ and $\nu_1 + \nu_2 + \nu_4 + \nu_5$ interacting levels

Florin Lucian Constantin

Laboratoire PhLAM, CNRS UMR 8523, 59655 Villeneuve d'Ascq, France

Email : FL.Constantin@univ-lille1.fr

Abstract

Calculations of the sensitivity to a variation of the electron-to-proton mass ratio μ for $^{12}\text{C}_2\text{H}_2$ transitions of the $\nu_1 + \nu_3$ and $\nu_1 + \nu_2 + \nu_4 + \nu_5$ bands in the spectral region at 1.5 μm are presented. They account for the Fermi and l-type rotation and vibration resonances of the excited states. The frequency splittings between near resonant transitions, arising from a cancellation of effective rotational intervals with frequency shifts associated to the vibrational band origin, the anharmonicity and the rotation-vibration interactions, have sensitivity coefficients to a variation of μ of both signs in the range of 10^{-10} . The measurements of temporal drifts of frequency splittings against the Cs frequency standard have the potential to better constrain a variation of μ comparing to that of other fundamental constants. The systematic frequency shifts for frequency splittings are discussed for experimental setups based on intracavity saturated absorption spectroscopy and the constraint of a measurement of a fractional variation of μ is projected at 10^{-10} level.

Keywords

electron-to-proton mass ratio constant variation; spectroscopic constants; Fermi and l-type interactions; rovibrational spectroscopy; acetylene frequency standard

Main body of the article

1. Introduction

The idea that fundamental constants may vary find new developments [1] within the context of modern theories. A possible variation of the fine structure constant should lead in the grand unification theories approaches to a variation of the strong interaction strength scale and masses. A fine tuning of the fundamental constants during cosmological time conducted to atoms and molecules that we know nowadays. Their energy levels may be investigated by high resolution spectroscopy to probe this variation. For different values of the fundamental constants, we would have different spectra, level-sensitive intra-molecular interactions, ionisation rates or chemical reactions. The electron to proton mass ratio μ is a fundamental constant that provides a scale of masses in quantum electrodynamics (QED) and quantum chromodynamics (QCD). Nuclear gyromagnetic factors g depend on quark masses and QCD strength scale [2]. Atomic hyperfine transitions are sensitive conjointly to variations of α , μ and g . Molecular rotational and rovibrational frequencies depend on inertia moments and nuclear masses that are intrinsically sensitive to a variation of μ . Measurements of different atomic transitions (see [3] for a review) lead to stringent constraints to a possible variation of α at $4 \times 10^{-16} \text{ yr}^{-1}$. Fractional variation of the electron-to-proton mass ratio μ is expected to be higher [4]. Probing a variation of μ with molecules has been performed by comparing molecular hydrogen electronic-rotation-vibration transitions measured in laboratory with the corresponding transitions detected in astrophysical objects at high redshift [5] or by comparing astrophysical spectra of ammonia rotation-inversion transitions with high sensitivity coefficients $K = (\Delta f/f)/(\Delta\mu/\mu)$ with rotational transitions [6]. Constraints on a fractional variation of μ have been tightened at 10^{-17} yr^{-1} level by exploiting methanol rotation-torsion transitions [7]. Alternative approaches were absolute frequency measurements in laboratory of molecular clocks based, for example, on ammonia rotation-inversion transitions detected in a fountain [8], respectively rovibrational transitions of trapped molecular hydrogen ions [9] or diatomic molecules in optical traps [10] and two-photon transitions on a molecular beam [11], that put constraints on a fractional variation of μ at $5.6 \times 10^{-14} \text{ yr}^{-1}$ level.

It has been shown that the splitting between near resonant energy levels has an enhanced sensitivity coefficient to a variation of μ . The measurements of transitions coupling such levels constrained a variation of the fundamental constants (see [12] for a review). For

example, vibrational energy in the ground electronic state may be cancelled by fine structure energy [13] or by vibrational energy in an excited electronic state [14-15]. An enhancement was suggested for the sensitivity coefficient of the frequency splitting between near resonant transitions of rotation or rotation-vibration from isotopic lithium hydride [16].

Acetylene displays strong combination bands in the spectral region at 1.5 μm . They have been addressed by Fourier transform spectroscopy [17], by using a multireflection cell [18], at high resolution [19] or by laser spectroscopy [20] to provide wavelength and frequency references. Saturated absorption spectroscopy using Fabry-Perot cavities was a step forward in the development of accurate frequency references [21]. Absolute frequency measurements of saturated absorption lines at kHz-level uncertainty were performed with frequency comb techniques. Theoretical developments based on an effective Hamiltonian accounting for sets of levels [22] allowed determination of accurate molecular parameters. This contribution addresses rovibrational transitions of $^{12}\text{C}_2\text{H}_2$ from the ground vibrational state to the $\nu_1 + \nu_3$ and $\nu_1 + \nu_2 + \nu_4 + \nu_5$ levels that are coupled by rotation-vibration interactions. The sensitivities of $^{12}\text{C}_2\text{H}_2$ transitions to a variation of μ are calculated here using an effective Hamiltonian for the interacting levels and a set of accurate molecular parameters. Near resonant transitions arise from the cancellation between rotational intervals and frequency shifts associated to the vibrational band origin, the anharmonicity or the rotation-vibration interactions. The sensitivity coefficient of the frequency splitting is also calculated and displays an increased value comparing to that of a transition. The absolute measurements of frequency splittings have the potential to better constrain a variation of μ comparing to a variation of other fundamental constants.

2. Acetylene rovibrational energy levels, transitions and sensitivities to a variation of μ

The vibrational energy levels are described in terms of normal modes and labelled as $\nu_1\nu_2\nu_3(\nu_4^{l_4}\nu_5^{l_5})^k$ where ν_s are quantum numbers of the vibrational normal modes, $l_{4,5}$ are angular momentum quantum numbers associated to the degenerate vibrational modes $\nu_{4,5}$ ($l_k = \pm \nu_k, \pm (\nu_k-2), \dots, \pm 1$ or 0). The rotational energy levels are described in the basis of angular momentum where the angular momentum quantum number is J and the quantum number of its projection of the molecular axis is $k = l_4 + l_5$. The rotational levels are positive (+), respectively negative (-) when the total eigenfunction remains unchanged, respectively changes of sign for an inversion. For isotopomers with a center of symmetry, vibrational energy levels are symmetric (g), respectively antisymmetric (u) with respect to an inversion. In addition, symmetry labels e, respectively f are used with the vibrational quantum numbers

to discriminate the parity of degenerate vibrational energy levels [23]: e levels have parity $+(-1)^J$ and f levels $-(-1)^J$.

Within the Born-Oppenheimer approximation, the diagonal terms of the Hamiltonian are written as a sum of a vibrational term and a rotational term. The vibrational term for the level $v = [v_1 v_2 v_3 (v_4^{l_4} v_5^{l_5})^k]$ is expressed as:

$$G_v[v] = \sum_s \omega_s (v_s + g_s/2) + \sum_{s \leq s'} x_{ss'} (v_s + g_s/2)(v_{s'} + g_{s'}/2) + \sum_{k \leq k'} g_{kk'} l_k l_{k'} \quad (1)$$

in terms of the normal mode frequency ω_s with degeneracy g_s ($g_1 = g_2 = g_3 = 1$, $g_4 = g_5 = 2$), the first-order anharmonicity $x_{ss'}$ and the first-order anharmonicity contribution of the degenerate bending modes $g_{kk'}$ ($k, k' = 4, 5$). The normal mode at frequency ω_1 is the CH symmetric stretching, at ω_2 is the CC symmetric stretching, at ω_3 is the CH asymmetric stretching, at ω_4 is the *trans* bending, respectively at ω_5 is the *cis* bending. The harmonic frequency ω_s^0 is defined in terms of the normal mode frequencies and the first-order anharmonicities:

$$\omega_s^0 = \omega_s + x_{ss} g_s + \sum_{s \neq s'} x_{ss'} g_{s'}/2 \quad (2)$$

The rotational term is expressed as:

$$F_r(J, k) = B[v](J(J+1) - k^2) - D[v](J(J+1) - k^2)^2 + H[v](J(J+1) - k^2)^3 \quad (3)$$

in terms of the effective rotational constant $B[v]$ and the quartic, respectively the sextic centrifugal distortion constants $D[v]$ and $H[v]$. The rotational constants are expressed in terms of the equilibrium constants B_e , D_e , H_e , respectively the ground-state constants B_0 , D_0 , H_0 and the first-order rotation-vibration constants α_s , β_s , h_s :

$$\begin{aligned} B[v] &= B_e - \sum_s \alpha_s (v_s + g_s/2) = B_0 - \sum_s \alpha_s v_s \\ D[v] &= D_e + \sum_s \beta_s (v_s + g_s/2) = D_0 + \sum_s \beta_s v_s \\ H[v] &= H_e + \sum_s h_s (v_s + g_s/2) = H_0 + \sum_s h_s v_s \end{aligned} \quad (4)$$

The values of α_s , β_s , h_s define the change of the equilibrium values of the rotational constant and centrifugal distortion constants due to the excitation of the s^{th} normal mode. They can be evaluated from the potential function for displacement of the atoms.

The effective Hamiltonian used in these calculations treats the interactions between the stretch-bend combination state $[11011^{2,0\pm}]$ of symmetry Σ_u^+ , Σ_u^- , $\Delta_u^{e,f}$ with the stretch combination state $[10100]$ of symmetry Σ_u^+ . Transitions discussed are from the Σ_g^+ ground state $[00000]$ to the $[11011^{0+}]$, respectively $[10100]$ Σ_u^+ states. Coupling of the $[110(1^1 1^1)^{0+}]$

and $[110(1^1 1^1)^{2e}]$ levels allows transitions from the ground state to the Δ_u^e level but they have not been observed. Information on the $\Delta_u^{e,f}$ level can be reached with transitions from excited states, for example from the bending fundamental $[00010] \Pi_g^{e,f}$ level. The vibrational l-type resonance couples the $[110(1^0 1^0)^{0e}]$ and $[110(1^1 1^1)^{0f}]$ levels and lifts their degeneracy. The off-diagonal term depends on the vibrational l-type doubling constant r_{45} expressed in function of the rotational quantum number as:

$$r_{45} = r_{045} + r_{J45}J(J+1) \quad (5)$$

The rotational l-type resonance couples the $[110(1^1 1^1)^0]$ and $[110(1^1 1^1)^2]$ levels with off-diagonal terms depending on the rotational l-type doubling constants q_k expressed in function of the rotational and vibrational quantum numbers as:

$$q_k = q_{0k} + q_{kk}v_k + q_{kk'}v_{k'} + q_{kJ}J(J+1) \quad (6)$$

with $k, k' = 4, 5$, $v_k = v_{k'} = 1$. The rotational l-type resonance adds to the $[110(1^1 1^1)^2]$ diagonal energy level a contribution depending on the Δ -state rotational l-type doubling constant ρ_{45} . The Fermi resonance couples the $[101(0^0 0^0)^{0e}]$ and $[110(1^1 1^1)^{0e}]$ levels with an off-diagonal term depending on the Fermi constant W expressed in function of the rotational quantum number as:

$$W = W_0 + W_{0J}J(J+1) \quad (7)$$

The first term is expressed as $W_0 = k_{2345}/4$ in function of an anharmonic interaction constant k_{2345} .

The Hamiltonian is diagonalized in blocks that have e and f symmetry. E-symmetry levels that can be addressed by rovibrational transitions from the ground state (e symmetry) are described by the following matrix:

$$\begin{pmatrix} E[110(1^1 1^1)^2, J] + \frac{\rho_{45}}{4}J(J+1)(J(J+1)-2) & \frac{q_4 + q_5}{2}\sqrt{J(J+1)(J(J+1)-2)} & 0 \\ \frac{q_4 + q_5}{2}\sqrt{J(J+1)(J(J+1)-2)} & E[110(1^1 1^1)^0, J] + r_{45} & W \\ 0 & W & E[101(0^0 0^0)^0, J] \end{pmatrix}$$

$$\begin{aligned} E[110(1^1 1^1)^2, J] &= (v_2 + g_{45}) + (B_2 + \gamma^{45})(J(J+1)-4) - (D_2 + \delta^{45})(J(J+1)-4)^2 + (H_2 + h^{45})(J(J+1)-4)^3 \\ E[110(1^1 1^1)^0, J] &= (v_2 - g_{45}) + (B_2 - \gamma^{45})J(J+1) - (D_2 - \delta^{45})(J(J+1))^2 + (H_2 - h^{45})(J(J+1))^3 \\ E[101(0^0 0^0)^0, J] &= v_1 + B_1J(J+1) - D_1(J(J+1))^2 + H_1(J(J+1))^3 \\ E[000(0^0 0^0)^0, J] &= B_0J(J+1) - D_0(J(J+1))^2 + H_0(J(J+1))^3 \end{aligned} \quad (8)$$

$B_{0,1,2}$, $D_{0,1,2}$, $H_{0,1,2}$ are the effective rotational constants for the $[00000]$, $[10100]$, respectively $[11011]$ vibrational levels, expressed using Eq. (4):

$$\begin{aligned}
B_1 &= B[10100] \\
B_2 &= B[11011] + \gamma^{44} + \gamma^{55} \\
D_1 &= D[10100] \\
D_2 &= D[11011] + \delta^{44} + \delta^{55} \\
H_1 &= H[10100] \\
H_2 &= H[11011] + h^{44} + h^{55}
\end{aligned} \tag{9}$$

where $\gamma^{kk'}$, $\delta^{kk'}$, $h^{kk'}$ are the rotation-vibration constants associated to the degenerate bending modes ($k, k' = 4, 5$) that add $l_k l_{k'}$ dependence to the corresponding effective rotational constants. The vibrational terms $v_{1,2}$ are the contributions of ω_s^0 , x_{ss} , g_{kk} to the vibrational energies:

$$\begin{aligned}
v_1 &= G_v[10100] \\
v_2 &= G_v[1101^0 1^0] + g_{44} + g_{55}
\end{aligned} \tag{10}$$

Each parameter A in the Hamiltonian has its own sensitivity to a variation of μ . The sensitivity coefficient K_A is defined as an adimensional quantity corresponding to the fractional variation of A for a given fractional variation of μ :

$$K_A = \frac{1}{A} \frac{dA}{d(\ln \mu)} \tag{11}$$

The main contributions to the energy levels arise from normal mode frequencies ω_s with a sensitivity coefficient $1/2$. The equilibrium rotational constant has a sensitivity coefficient of 1. The higher order terms of the Hamiltonian have been expressed on basic molecular parameters, normal mode frequencies and rotational constants [22,24-27] allowing to derive their sensitivity coefficients. The anharmonicity adding $v_s v_{s'}$ and $l_k l_{k'}$ dependences to the vibrational term has a sensitivity coefficient of 1. The quartic and sextic equilibrium centrifugal distortion constants have a sensitivity coefficient of 2, respectively 3. The sensitivity coefficients for rotation-vibration constants involved in the expression of the effective rotational constants are: $3/2$ for α_s adding v_s dependence, 2 for $\gamma^{kk'}$ adding $l_k l_{k'}$ dependence. The sensitivity coefficients for rotation-vibration constants involved in the expression of the effective quartic centrifugal distortion constants are: $5/2$ for β_s adding v_s dependence, 3 for $\delta^{kk'}$ adding $l_k l_{k'}$ dependence. The vibrational l-type resonance constant r_{045} has a sensitivity coefficient of 1, r_{J45} adding $J(J+1)$ dependence has a sensitivity coefficient of 2. The rotational l-type resonance constant q_{0k} has a sensitivity coefficient of $3/2$. The sensitivity coefficients for higher-order terms are: 2 for $q_{kk'}$ adding v_k dependence, $5/2$ for q_{kJ} adding $J(J+1)$ dependence. The term ρ_{45} adding $[J(J+1)]^2 - 2[J(J+1)]$ dependence has a sensitivity coefficient of 2. The Fermi interaction term W_0 has a sensitivity coefficient of 1 and the term W_{0J} adding $J(J+1)$ dependence has a sensitivity coefficient of 2.

The parameters used in the calculations are listed in Table 1. Accurate ground state rotational constants are from [28], the Fermi and l-type interaction constants are those determined in [29,30] by fitting the similar interaction between [00100] and [01011] levels, the anharmonicities from [31], the rotation-vibration constants α_s are from [32] and $\gamma^{kk'}$ are from [29,30] determined by global fits, while band centers, respectively the rotational constants and quartic distortion constants in the excited states are fixed to the values fitted in [33]. Accurate rotation-vibration constants β_s , $\delta^{kk'}$ are from [34] determined by global fits and the sextic centrifugal distortion constants in the excited states are fixed to the ground state value from [28]. For most parameters Fourier Transform spectroscopy measurements were used and wavenumbers are converted in frequency units. The calculations neglect the higher-order anharmonicities, the rotation-vibration constants adding $v_s v_{s'}$ dependence or higher-order dependences for the rotational constants or for the quartic centrifugal distortion constants, respectively the rotation-vibration constants for the sextic centrifugal distortion constants. Fig. 1 displays a plot of the energy levels calculated using diagonal term values and the transitions addressing these levels from the ground state.

The sensitivities of $v_{1,2}$ are calculated with Eqs. (1) and (10) as a linear dependence on $v_{1,2}$, $x_{ss'}$, $g_{kk'}$, by expanding $v_{1,2}$ in function of ω_s with a sensitivity coefficient of $1/2$ and of $x_{ss'}$, $g_{kk'}$ with a sensitivity coefficient of 1. The uncertainty of the sensitivity of $v_{1,2}$ is calculated by quadratically adding the terms of the previous dependence expressed in function of $v_{1,2}$, $x_{ss'}$, $g_{kk'}$ uncertainties. The uncertainty of the sensitivity is determined mainly by $x_{ss'}$, $g_{kk'}$ uncertainties. The fractional uncertainty of the sensitivity coefficient is estimated at $\sim 10^{-4}$, by quadratically adding the fractional uncertainties of the vibrational term and of its sensitivity. The sensitivities of $B_{0,1,2}$ and $D_{0,1,2}$ are calculated with Eqs. (4) and (9) as a linear dependence on $B_{0,1,2}$, α_s , γ^{kk} respectively $D_{0,1,2}$, β_s , δ^{kk} by expanding $B_{0,1,2}$, $D_{0,1,2}$ in function of B_e , D_e with sensitivity coefficients of 1, respectively 2, of α_s , β_s with sensitivity coefficients of 1.5, respectively 2.5 and of γ^{kk} , δ^{kk} with sensitivity coefficients of 2, respectively 3. The uncertainty of the sensitivity of $B_{0,1,2}$, $D_{0,1,2}$ calculated by quadratically adding the terms of the previous dependence expressed in function of $B_{0,1,2}$, α_s , γ^{kk} respectively $D_{0,1,2}$, β_s , δ^{kk} uncertainties, is determined mainly by the uncertainties of the rotation-vibration constants. The fractional uncertainty of the sensitivity coefficient is estimated for B_0 at 4×10^{-7} and $B_{1,2}$ at 10^{-6} , respectively for D_0 at 2×10^{-5} , D_1 at $\sim 10^{-4}$ and D_2 at $\sim 2 \times 10^{-3}$ by quadratically adding the fractional uncertainties of the rotational constant and of its sensitivity.

The sensitivity, respectively the sensitivity coefficient of a rovibrational transition are expressed as:

$$\begin{aligned} df/d(\ln \mu) &= dE'[v', J']/d(\ln \mu) - dE''[v'', J'']/d(\ln \mu) \\ K &= d(\ln f)/d(\ln \mu) = (dE'[v', J']/d(\ln \mu) - dE''[v'', J'']/d(\ln \mu)) / (E'[v', J'] - E''[v'', J'']) \end{aligned} \quad (12)$$

in terms of the higher $E'[v', J']$, respectively the lower $E''[v'', J'']$ rovibrational energy. For a pair of two transitions at higher f_1 , respectively lower f_2 frequency, a similar formula can be written for the sensitivity, respectively the sensitivity coefficient of the frequency splitting $X = f_1 - f_2$:

$$\begin{aligned} dX/d(\ln \mu) &= df_1/d(\ln \mu) - df_2/d(\ln \mu) \\ K &= d(\ln X)/d(\ln \mu) = (df_1/d(\ln \mu) - df_2/d(\ln \mu)) / (f_1 - f_2) \end{aligned} \quad (13)$$

The expression suggests an increased sensitivity coefficient for the splitting between near resonant transitions with different sensitivities.

3. Experimental approach

Acetylene transitions were used as frequency references at 1.5 μm . Doppler-free saturated absorption spectroscopy benefited from developments of diode lasers or fiber lasers with high intrinsic spectral purity in this spectral region. Probing the transition in a Fabry-Perot cavity allowed an enhancement of the molecular signal contrast [21]. The excellent metrological performances of the setup were recognized by the *Comité International des Poids et Mesures* that recommended P(16) transition of the $^{13}\text{C}_2\text{H}_2$ $v_1 + v_3$ band as the reference for absolute frequency in this spectral region [35]. Absolute frequency measurements of acetylene reference transitions were performed using frequency combs at National Physical Laboratory (NPL) [36], National Research Council of Canada (NRC) [37], National Metrology Institute of Japan (NMIJ) [38]. In addition, measurements of frequency intervals between a reference line and unknown molecular lines lead to grids of absolute frequencies for the $v_1 + v_3$ band lines of $^{12}\text{C}_2\text{H}_2$ [28,39] and $^{13}\text{C}_2\text{H}_2$ [40,41] and for the $v_1 + v_2 + v_4 + v_4$ band lines of $^{13}\text{C}_2\text{H}_2$ [40].

The experimental setup is based on a laser source that is phase-modulated with an external electro-optic modulator and stabilized by the Pound-Drever-Hall method on a resonance of a Fabry-Perot cavity filled with acetylene. The cavity length is modulated with a piezo-electric ceramic and the transmitted signal is demodulated at the third harmonic to lock the cavity length on the saturated absorption line. Typical performances are a laser linewidth of tens of kHz, a fractional stability of a few 10^{-12} at 1 s and a frequency reproducibility of ~ 1 kHz.

Consider two independent systems locked on near resonant transitions. The beatnote between the lasers can be recorded with a fast detector and counted against the signal of a Cs primary frequency standard. The fractional time variation of the frequency ratio between the frequency splitting X and the clock frequency f_{Cs} due to the fractional time variation of the fundamental constants is expressed as:

$$\frac{d \ln(X / f_{Cs})}{dt} = (d_{\mu} \ln X - 1) \frac{d \ln \mu}{dt} - (2 + A_{HFS}(Cs)) \frac{d \ln \alpha}{dt} - \frac{d \ln g_{Cs}}{dt} \quad (14)$$

This dependence includes the fractional time variation of Cs reference frequency [42] in terms of the fractional time variation of α , where $A_{HFS} \sim 0.83$ [2], μ and Cs g-factor g_{Cs} . A small linear time variation of the fundamental constants contributes to a small linear time dependence the frequency ratio with a slope depending on the sensitivity coefficient $d_{\mu} \ln X$, respectively on $A_{HFS}(Cs)$.

The typical statistic uncertainty of the frequency splitting is estimated at 1 kHz. Frequency splittings of near resonant transitions of some GHz with sensitivity coefficients by 10^2 can be measured at a given time with a fractional frequency uncertainty by 10^{-7} . If the measurement is repeated in time, a frequency drift that may be observed with this method leads to tighter constraints on the fractional time variation of μ than on the fractional time variation of α , g_{Cs} because of the enhanced sensitivity coefficient. The significance of a frequency drift should be verified by cautiously accounting the systematic effects.

Systematic frequency shifts were measured for a few lines [28,39-41]. It is expected that other acetylene lines have the same sensitivities to experimental parameters. The systematic effects for a frequency splitting may be easily derived from those of each line and it is anticipated that their absolute value is generally smaller.

Power shifts of some reference lines have comparable values. A power shift of -1.5 kHz/(W/mm²) for ¹³C₂H₂ measured at NPL [40] corresponds to a frequency shift of -0.3 kHz, that is comparable with the result of -11.4 kHz/W at NRC [41] leading to a shift of -1.4 kHz. Assuming an uncertainty of 5% of the intracavity laser power allows to estimate power shift uncertainties of 0.015 kHz, respectively 0.068 kHz. For ¹²C₂H₂, the result at NPL [28] of -3.2 kHz/(W/mm²) leads to -0.9 kHz systematic shift with an estimated uncertainty of 0.045 kHz.

Pressure shifts measured by linear spectroscopy depend strongly on the line but have the same sign. The pressure shift for ¹²C₂H₂ [43] increases linearly with J in the R branch, ranging from -1.05 kHz/Pa to -5.48 kHz/Pa and maintains a value of -2.18 kHz/Pa for the most of P branch lines. The systematic shift for a frequency splitting can be estimated by assuming that the

$\nu_1 + \nu_3$ and $\nu_1 + \nu_2 + \nu_4 + \nu_5$ bands have the same J dependence of the pressure shift. For example, the systematic effect on the frequency splitting between the Doppler lines R(18) of $\nu_1 + \nu_3$ band and P(11) of $\nu_1 + \nu_2 + \nu_4 + \nu_5$ band is estimated at 1.9 kHz/Pa, that is smaller than the absolute value of the pressure shift of each line. A linear shift with J is measured for $^{13}\text{C}_2\text{H}_2$ lines [44] with a slope of -0.1 kHz/Pa for the P branch and -0.24 kHz/Pa for the R branch. Measurements at NRC by saturated absorption spectroscopy lead to a pressure shift for the $^{13}\text{C}_2\text{H}_2$ reference transition of -1.73 kHz/Pa [37], compatible with the result obtained by linear spectroscopy. Dependences of the pressure shift on the rotational quantum number, P, R branch or vibrational band were not observed with the experimental setup at NPL [40]. Assuming a measurement at 3 Pa with a fractional uncertainty of 3.3%, the pressure shift estimated for the reference transition is -5.18 kHz with an uncertainty of 0.173 kHz. The pressure shift measured at NPL by exchanging sealed cells is 0.5 kHz/Pa and leads to an uncertainty of 0.050 kHz.

The second-order Doppler effect (SODE) induces a frequency shift proportionally with the square of the mean velocity. The SODE shifts for reference transitions measured in a cell maintained at 300 K are estimated at -0.208 kHz for $^{12}\text{C}_2\text{H}_2$, respectively -0.193 kHz for $^{13}\text{C}_2\text{H}_2$. A temperature uncertainty of 0.5 K leads to a SODE shift uncertainty of 0.3 Hz.

On the other hand, the frequency shift associated to the low-frequency modulation depth depends specifically on the laser system, ranging from -0.3 kHz/MHz [28] to 4.7 kHz/MHz [37]. Assuming a fractional uncertainty of the modulation depth of 5%, the uncertainty of the modulation shift is estimated from 0.08 kHz [28] to 0.5 kHz [39]. Moreover, electric offsets in the detection system lead to frequency shifts with uncertainties estimated at ~0.010 kHz from results at NPL [28] to 0.5 kHz at NRC [39,41].

All above systematic effects are quadratically added to estimate an uncertainty for the $^{13}\text{C}_2\text{H}_2$ reference transition of 0.096 kHz measured with the experimental setup at NPL, respectively of 0.731 kHz at NRC. Consider a frequency splitting measured using two similar systems with the same uncertainty of the experimental parameters. The uncertainty of the frequency splitting depends on the difference of the sensitivities of acetylene lines of each system to the experimental parameters. A proper estimation of the uncertainty requires extensive measurements of the sensitivities of each line to the experimental parameters that have not been performed yet. Moreover, the uncertainty may be reduced, as the partial contributions of the power shifts may be cancelled for example by a proper balance of laser power. Typical systematic frequency uncertainty of the frequency splittings is estimated here as the same as that of the reference transition for the experimental setup at NPL [36]. For frequency

splittings of some GHz with sensitivity coefficients of $\sim 10^2$, the systematic effects constraint the fractional uncertainty of a measurement of a variation of μ at 10^{-10} level. The constraint on the fractional variations of α , g_{Cs} is by two orders of magnitude smaller. Measuring the temporal drift of the difference between two equal frequency splittings with sensitivity coefficients of opposite signs by $\pm 10^2$ is attractive because it allows to discriminate a fractional variation of μ at $\sim 7 \times 10^{-11}$ against any variation of α , g_{Cs} .

The fractional statistic uncertainty of the frequency splitting is estimated here with the fractional Allan variance of the $^{13}\text{C}_2\text{H}_2$ reference transition [36]. For a frequency splitting of 1 GHz, the dependence is $\sim 4.4 \times 10^{-7} \tau^{-1/2}$ on the measurement time τ in seconds. The fractional statistic uncertainty may be reduced by a factor of 3.6×10^{-2} by increasing the time of the measurement to reach the Allan variance plateau at $\tau \sim 4000$ s. The measurement of a frequency splitting with a sensitivity coefficient of 10^2 determines a quantity proportional with μ with a fractional statistic uncertainty of 1.6×10^{-10} for this model of rovibrational energy levels.

4. Results and discussion

4.1. Sensitivity of rovibrational transitions

The Hamiltonian matrix is calculated for e-symmetry levels for each J value and numerically diagonalized. The model is used to predict frequencies of the $\nu_1 + \nu_3$ respectively $\nu_1 + \nu_2 + \nu_4 + \nu_5$ band transitions for J up to 30. The shift between the calculated frequencies of the $\nu_1 + \nu_3$ band transitions and the experimental frequencies from [28], measured with an accuracy of ~ 1 kHz, is less than 0.9 GHz. For the $\nu_1 + \nu_2 + \nu_4 + \nu_5$ band transitions measured in [33] (supplementary material [34]) with an accuracy of ~ 12 GHz, the shift is less than 5 GHz.

Molecular constants are incremented in proportion with their sensitivity coefficients for a fractional variation of μ of 10^{-7} . Sets of μ -dependent values of rovibrational frequencies are calculated and the sensitivities are derived as the slope of the dependence on the fractional variation of μ .

It is interesting to discuss contributions of different terms to the sensitivity of rovibrational transitions. Diagonal terms are approximated as the sum between $J(J + 1) - k^2$ dependence with the rotational constants B_1 , $B_{22,20} = B_2 \pm \gamma^{45}$ and the corresponding vibrational terms ν_1 , $\nu_{22} = \nu_2 + g_{45} - 4B_2$, $\nu_{20} = \nu_2 - g_{45} + r_{45}$. Contributions of the non-diagonal terms, expressed as $W = k_{2345}/4$ and $Q(J) = [(q_4 + q_5)/2] \times [J(J + 1)(J(J + 1) - 2)]^{1/2}$, are estimated by second-order

perturbation theory as $W, Q(J) \ll v_{1,20,22} + B_{1,20,22}J(J + 1)$. The contribution of the l-type rotational resonance is a shift of the $[110(1^11^1)^2]$ and $[110(1^11^1)^{0+}]$ rotational levels by $Q^2(J)/\Delta^{02}$, respectively $-Q^2(J)/\Delta^{02}$, where $\Delta^{02} = v_{22} - v_{20} = 2g_{45} - r_{45} - 4B_2 = 448$ GHz. The shift is comparable with the contribution of the centrifugal distortion to the diagonal rovibrational energy. The Fermi interaction shifts the $[110(1^11^1)^{0+}]$ and $[10100]$ levels by W^2/Δ_{12} , respectively $-W^2/\Delta_{12}$, where $\Delta_{12} = v_{20} - v_1 = v_2 - g_{45} + r_{45} - v_1 = 1.96$ THz. The shift corresponds to about a half of the rotational interval. Perturbed energy levels $E_{i,per}$ are expressed with $v_{i,per}$, $B_{i,per}$ at the first order in $J(J + 1)$ as $(B_{22} - B_{20})J(J + 1) \ll \Delta^{02}$ and $(B_{20} - B_1)J(J + 1) \ll \Delta_{12}$, leading to the following expressions:

$$\begin{aligned}
E_{i,per}[J] &= v_{i,per} + B_{i,per}J(J + 1); \\
v_{22,per} &= v_{22} + \left(\frac{Q(J)}{\Delta^{02}}\right)^2 \Delta^{02}; B_{22,per} = B_{22} - \left(\frac{Q(J)}{\Delta^{02}}\right)^2 (B_{22} - B_{20}); \\
v_{20,per} &= v_{20} - \left(\frac{Q(J)}{\Delta^{02}}\right)^2 \Delta^{02} + \left(\frac{W}{\Delta_{12}}\right)^2 \Delta_{12}; B_{20,per} = B_{20} - \left(\frac{Q(J)}{\Delta^{02}}\right)^2 (B_{20} - B_{22}) - \left(\frac{W}{\Delta_{12}}\right)^2 (B_{20} - B_1); \\
v_{1,per} &= v_1 - \left(\frac{W}{\Delta_{12}}\right)^2 \Delta_{12}; B_{1,per} = B_1 - \left(\frac{W}{\Delta_{12}}\right)^2 (B_1 - B_{20});
\end{aligned} \tag{15}$$

Rovibrational frequencies in the $v_1 + v_3$ and $v_1 + v_2 + v_4 + v_5$ bands are expressed as:

$$\begin{aligned}
f_{13}(m) &= v_{1,per} + (B_{1,per} + B_0)m + (B_{1,per} - B_0)m^2 \\
f_{1245}(m) &= v_{20,per} + (B_{20,per} + B_0)m + (B_{20,per} - B_0)m^2
\end{aligned} \tag{16}$$

where $m(J)$ is an integer assigned to each transition such that $m = J + 1$ for R branch and $m = -J$ for P branch. When perturbations are neglected, the rovibrational frequencies are expressed as the sum between a vibrational term with a sensitivity coefficient of $\sim 1/2$, a linear term in $m(J)$ with a sensitivity coefficient of ~ 1 and a quadratic term in $m(J)$ with a sensitivity coefficient of ~ 1.5 . The Fermi interaction shifts rovibrational frequencies of the $v_1 + v_3$ band by an interval $-W^2/\Delta_{12} \sim -18$ GHz. The absolute value of this frequency shift has a sensitivity coefficient of ~ 1.7 . The contribution to the rotational constant is to add a term $-(W/\Delta_{12})^2(B_1 - B_{20}) \sim 1.2$ MHz with a sensitivity coefficient of ~ 2.8 . At low J , the rotational l-type interaction brings negligible contributions to the $v_1 + v_2 + v_4 + v_5$ rovibrational band frequencies comparing to those arising from the Fermi interaction. The result is symmetric to that observed in the $v_1 + v_3$ band, that is a shift of rovibrational frequencies by an interval ~ 18 GHz with a sensitivity coefficient of ~ 1.7 and a change of the rotational constant by a term ~ 1.2 MHz. Its absolute value has a sensitivity coefficient of ~ 2.8 . The contribution of the rotational l-type interaction increases quadratically with J to reach the order of magnitude of that of the Fermi interaction at high J . It consists in a negative shift of the $v_1 + v_2 + v_4 + v_5$

rovibrational band frequencies with a sensitivity coefficient of ~ 2 and a negative change of the rotational constant with a sensitivity coefficient of ~ 2.5 .

4.2 Sensitivity of frequency splittings between rovibrational transitions

Consider an anchor rovibrational transition in the $\nu_1 + \nu_3$ band at $f_{13}(m)$ and the same transition at $f_{1245}(m)$ probed in the $\nu_1 + \nu_2 + \nu_4 + \nu_5$ band. The vibrational shift, defined as the splitting between these transitions, is expressed using Eq. (15) as:

$$f_{1245}(m) - f_{13}(m) = (\nu_{20,per} - \nu_{1,per}) + (B_{20,per} - B_{1,per})m + (B_{20,per} - B_{1,per})m^2 \quad (17)$$

The difference between the perturbed vibrational terms, respectively the perturbed rotational constants, involves two times the contribution from the Fermi interaction and the $J(J + 1)$ dependent contribution from the l-type rotational resonance as discussed above. Near resonant transitions at $f_{1245}(m)$ and $f_{13}(m')$ are found when the vibrational shift equals the frequency splitting between different rovibrational transitions in the $\nu_1 + \nu_3$ band that is expressed as:

$$f_{13}(m') - f_{13}(m) = (m' - m) \times [(B_{1,per} + B_0) + (B_{1,per} - B_0)(m + m')] \quad (18)$$

Comparison of Eqs. (17) and (18) suggests that near resonant transitions are in R or P branches of the $\nu_1 + \nu_3$ band at low absolute value of m' and the P branch of the $\nu_1 + \nu_2 + \nu_4 + \nu_5$ band at high absolute value of m , where contributions of interactions cannot be neglected. Alternatively, near resonant transitions are found in the R branch of the $\nu_1 + \nu_3$ band for intermediate m' and in the P branch of the $\nu_1 + \nu_2 + \nu_4 + \nu_5$ band for intermediate absolute value of m .

Fig. 2 displays the dependence on the rotational quantum number of the sensitivity coefficient of the frequency splitting between near resonant transitions: P(J) of the $\nu_1 + \nu_3$ band and P(25 + J) of the $\nu_1 + \nu_2 + \nu_4 + \nu_5$ band, with a minimum of -1265 at $J = 4$, respectively R(J) of the $\nu_1 + \nu_3$ band and P(25 - J) of the $\nu_1 + \nu_2 + \nu_4 + \nu_5$ band and R(J) of the $\nu_1 + \nu_3$ band and P(29 - J) of the $\nu_1 + \nu_2 + \nu_4 + \nu_5$ band, with a maximum of 681 at $J = 18$. If the dependence of the sensitivity to a variation of μ on the calculated frequencies for the vibrational bands (shown in Fig. 3) is considered, the sensitivity coefficient corresponds to the slope of the line connecting data points, that have an increased value for near resonant transitions. Although the frequency splitting is always positive, the sensitivity coefficient may be positive or negative, that imply an increase, respectively a decrease of the frequency splitting with an increase of μ . The sensitivity coefficient varies rapidly around its extreme values when J changes by one unit for each transition.

4.3 Prospective for measurements of a variation of μ

Consider the measurement of the frequency drift of the $^{12}\text{C}_2\text{H}_2$ P(16) reference transition of the $\nu_1 + \nu_3$ band, with a sensitivity coefficient of 0.468, against the Cs frequency standard. The systematic uncertainties, estimated as above, constraint the measurement of a variation of μ at 9.43×10^{-13} , if the variations of α , g_{Cs} are neglected. The measurement of the drift of the frequency splitting between R(18) of the $\nu_1 + \nu_3$ band and P(11) of the $\nu_1 + \nu_2 + \nu_4 + \nu_5$ band with a sensitivity coefficient of 681.16 constraint a variation of μ at 1.34×10^{-10} . Measurements of transitions at higher frequency may tighten the constraint, despite the fact that the frequency splittings are greater and their sensitivity coefficients are smaller. For example, the measurement of the drift of the frequency splitting between R(30) of the $\nu_1 + \nu_3$ band and P(3) of the $\nu_1 + \nu_2 + \nu_4 + \nu_5$ band with a sensitivity coefficient of -61.16 constraint a variation of μ at 1.13×10^{-10} . The measurement of the drift of the frequency splitting between P(2) of the $\nu_1 + \nu_2 + \nu_4 + \nu_5$ band and R(30) of the $\nu_1 + \nu_3$ band with a sensitivity coefficient of 15.69 constraint also a variation of μ at 1.13×10^{-10} . The comparison of the last two measurements may discriminate a variation of μ at 9×10^{-11} .

5. Conclusion

This article presents calculations of the sensitivity of rovibrational transitions of the $^{12}\text{C}_2\text{H}_2$ of $\nu_1 + \nu_3$ and $\nu_1 + \nu_2 + \nu_4 + \nu_5$ bands to a variation of μ . They provide frequency references in the spectral region at 1.5 μm with sub-kHz level accuracy ($\sim 10^{-12}$ of the absolute frequency) with experimental setups based on intracavity saturated absorption spectroscopy. It is shown that the frequency splitting between near resonant transitions has an enhanced sensitivity coefficient. Such degeneracy arise at the lowest approximation order from the cancellation of effective rotational intervals with frequency shifts associated to the vibrational band origin, the anharmonicity, the Fermi and l-type rotational and vibrational interactions. The measurements of temporal drifts of frequency splittings against the Cs standard have the potential to better constrain a variation of μ comparing to that of α , g_{Cs} by exploiting high sensitivity coefficients to a variation of μ of both signs. Pairs of near resonant transitions with sensitivity coefficients in the range 10 - 10^3 are identified. The frequency splittings can be measured with statistic fractional uncertainties better than 10^{-7} . Systematic effects on frequency splittings are discussed for experimental setups at NPL [28,40] and NRC [39,41] and the uncertainty for a measurement of a fractional variation of μ is projected at 10^{-10} level.

References

- [1] J. -P. Uzan, *Rev. Mod. Phys.* 75, 403 (2003).
- [2] V. V. Flambaum and A. F. Tedesco, *Phys. Rev. C* 73, 055501 (2006).
- [3] S. N. Lea, *Eur. Phys. J. Special Topics* 163, 37 (2008).
- [4] X. Calmet and H. Fritzsch, *Eur. Phys. J. C* 24, 639 (2002).
- [5] E. Reinhold, R. Buning, U. Hollenstein, P. Petitjean, A. Ivanchik and W. Ubachs, *Phys. Rev. Lett.* 96, 151101 (2006).
- [6] V. V. Flambaum and M. G. Kozlov, *Phys. Rev. Lett.* 98, 240801 (2007).
- [7] J. Bagdonaite, P. Jansen, C. Henkel, H. L. Bethlem, K. M. Menten and W. Ubachs, *Science* 339, 46 (2013).
- [8] H. L. Bethlem, M. Kajita, B. Sartakov, G. Meijer and W. Ubachs *Eur. Phys. J. Special Topics* 163, 55 (2008).
- [9] S. Schiller and V. Korobov, *Phys. Rev. A* 71, 032505 (2005).
- [10] M. Kajita, *Phys. Rev. A* 84, 022507 (2011).
- [11] A. Shelkovich, R. J. Butcher, C. Chardonnet and A. Amy-Klein, *Phys. Rev. Lett.* 100, 150801 (2008).
- [12] P. Jansen, H. L. Bethlem and W. Ubachs, *J. Chem. Phys.* 140, 010901 (2014).
- [13] V. V. Flambaum and M. G. Kozlov, *Phys. Rev. Lett.* 99, 150801 (2007).
- [14] D. DeMille, S. Sainis, J. Sage, T. Bergeman, S. Kotochigova and E. Tiesinga, *Phys. Rev. Lett.* 100, 043202 (2008).
- [15] T. Zelevinski, S. Koyochigova and J. Ye, *Phys. Rev. Lett.* 100, 043201 (2008).
- [16] F. L. Constantin, *J. Phys. B: At. Mol. Opt. Phys.* 48, 175006 (2015).
- [17] A. Baldacci, S. Gherseti and K. Narahari Rao, *J. Mol. Spectrosc.* 68, 183 (1977).
- [18] B. C. Smith and J. S. Winn, *J. Chem. Phys.* 89, 4638 (1988).
- [19] Q. Kou, G. Guelachvili, A. Tamsamani and M. Herman, *Can. J. Phys.* 72, 1241 (1994).
- [20] T. Yoshida and H. Sasada, *J. Mol. Spectrosc.* 153, 208 (1992).
- [21] M. de Labachellerie, K. Nakagawa and M. Ohtsu, *Opt. Lett.* 19, 840 (1994).
- [22] J. Pliva, *J. Mol. Spectrosc.* 44, 165 (1972).
- [23] J. M. Brown, J. T. Hougen, K. P. Huber, J. W. C. Johns, I. Kopp, H. Lefebvre-Brion, A. J. Merer, D. A. Ramsay, J. Rostas and R. M. Zare, *J. Mol. Spectrosc.* 55, 500 (1975).
- [24] D. Papousek and M. R. Aliev, "Molecular Vibrational-Rotational Spectra," Elsevier Scientific Publishing Company: New York, 1982.
- [25] J. K. G. Watson, *J. Mol. Spectrosc.* 101, 83 (1983).
- [26] T. Nakagawa and Y. Morino, *J. Mol. Spectrosc.* 31, 208 (1969).

- [27] G. Amat and H. H. Nielsen, *J. Mol. Spectrosc.* 2, 152 (1958).
- [28] C. S. Edwards, G. P. Barwood, H. S. Margolis, P. Gill and W. R. C. Rowley, *J. Mol. Spectrosc.* 234, 143 (2005).
- [29] Y. Kabbadj, M. Herman, G. Di Lonardo, L. Fusina and J. W. C. Johns, *J. Mol. Spectrosc.* 150, 535 (1991).
- [30] J. Vander Auwera, D. Hurtmans, M. Carleer and M. Herman, *J. Mol. Spectrosc.* 157, 337 (1993).
- [31] M. I. El Idrissi, J. Liévin, A. Campargue and M. Herman, *J. Chem. Phys.* 110, 2074 (1999).
- [32] M. Herman, A. Campargue, M. I. El Idrissi and J. Vander Auwera, *J. Phys. Chem. Ref. Data* 32, 921 (2003).
- [33] K. A. Keppler, G. C. Mellau, S. Klee, B. P. Winnewisser, M. Winnewisser, J. Pliva and K. N. Rao, *J. Mol. Spectrosc.* 175, 411 (1996).
- [34] S. Robert, M. Herman, A. Fayt, A. Campargue, S. Kassi, A. Liu, L. Wang, G. Di Lonardo and L. Fusina, *Mol. Phys.* 106, 2581 (2008).
- [35] T. J. Quinn, *Metrologia* 40, 103 (2003).
- [36] C. S. Edwards, H. S. Margolis, G. P. Barwood, S. N. Lea, P. Gill, G. Huang and W. R. C. Rowley, *Opt. Lett.* 29, 566 (2004).
- [37] A. Czajkowski, A. A. Madej and P. Dube, *Opt. Commun.* 234, 259 (2004).
- [38] F. -L. Hong, A. Onae, J. Jiang, R. Guo, H. Inaba, K. Minoshima, T. R. Schibli, H. Matsumoto and K. Nakagawa, *Opt. Lett.* 28, 2324 (2003).
- [39] A. A. Madej, A. J. Alcock, A. Czajkowski, J. E. Bernard and S. Chepurov, *J. Opt. Soc. Am. B* 23, 2200 (2006).
- [40] C. S. Edwards, H. S. Margolis, G. P. Barwood, S. N. Lea, P. Gill and W. R. C. Rowley, *Appl. Phys. B* 80, 977 (2005).
- [41] A. A. Madej, J. E. Bernard, A. J. Alcock, A. Czajkowski and S. Chepurov, *J. Opt. Soc. Am. B* 23, 741 (2006).
- [42] E. Peik, B. Lipphardt, H. Schnatz, T. Schneider, C. Tamm and S. G. Karshenboim, *Phys. Rev. Lett.* 93, 170801 (2004).
- [43] W. C. Swann and S. L. Gilbert, *J. Opt. Soc. Am. B* 17, 1263 (2000).
- [44] M. Kusaba and J. Henningsen, *J. Mol. Spectrosc.* 209, 216 (2001).

Figure Captions

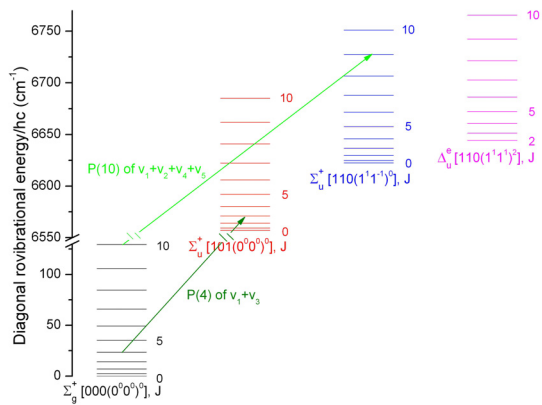


Fig. 1 Rovibrational energy levels calculated with diagonal terms of the Hamiltonian for $J = 0 - 10$. Some transitions pertaining to selected pairs of near resonant transitions discussed below.

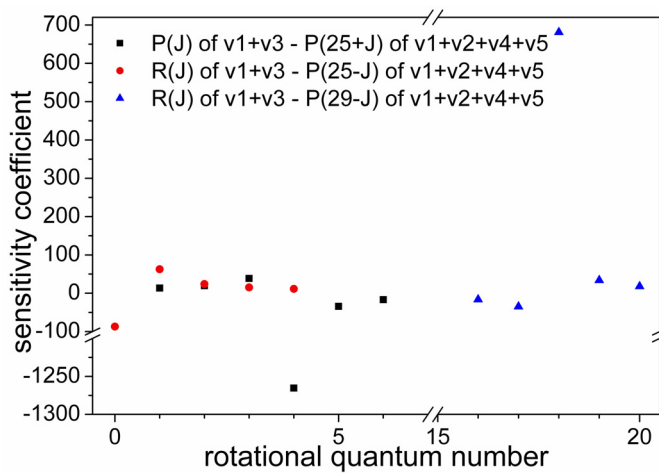


Fig. 2 Dependence of the sensitivity coefficient for the selected pairs of near resonant transitions on the rotational quantum number of the $v_1 + v_3$ band transition.

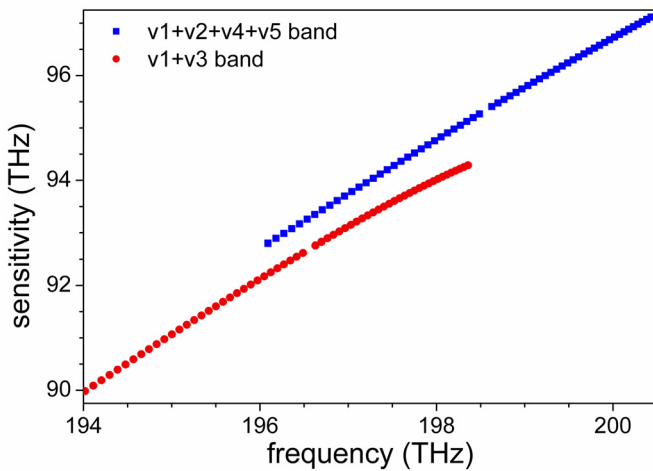


Fig. 3 Dependence of the sensitivity of the $v_1 + v_3$ and $v_1 + v_2 + v_4 + v_5$ band transitions on the calculated rovibrational frequency.

Table Captions

Table 1 Parameters of the rovibrational Hamiltonian and their sensitivity coefficients.

Constant	Value (GHz)	K_A	Constant	Value (GHz)	K_A
B_0	35.274974565(42)	0.9974937(4)	x_{14}	-416.1(42)	1
$D_0 (\times 10^6)$	48.77824(39)	2.01457(5)	x_{15}	-315.4(48)	1
$H_0 (\times 10^{12})$	57(18)	3	x_{22}	-223.4(21)	1
$\alpha_1 (\times 10^3)$	206.986(33)	1.5	x_{23}	-184.7(33)	1
$\alpha_2 (\times 10^3)$	185.308(39)	1.5	x_{24}	-381.6(30)	1
$\alpha_3 (\times 10^3)$	176.332(33)	1.5	x_{25}	-45.9(22)	1
$\alpha_4 (\times 10^3)$	-40.5780(26)	1.5	x_{33}	-828.3(36)	1
$\alpha_5 (\times 10^3)$	-66.9159(12)	1.5	x_{34}	-300.4(42)	1
$\gamma^{44} (\times 10^4)$	-19.720(33)	2	x_{35}	-280.0(48)	1
$\gamma^{55} (\times 10^4)$	-32.954(15)	2	x_{44}	103.7(16)	1
$\gamma^{45} (\times 10^4)$	-67.641(12)	2	x_{45}	-66.9(30)	1
$\beta_1 (\times 10^8)$	-42.45(27)	2.5	x_{55}	-71.2(16)	1
$\beta_2 (\times 10^8)$	5.93(44)	2.5	g_{44}	23.42939(27)	1
$\beta_3 (\times 10^8)$	-40.99(40)	2.5	g_{45}	198.00315(24)	1
$\beta_4 (\times 10^8)$	103.13(23)	2.5	g_{55}	104.21008(19)	1
$\beta_5 (\times 10^8)$	77.76(18)	2.5	r_{45}	-187.03212(33)	1
$\delta^{44} (\times 10^{10})$	-517(18)	3	$r_{J45} (\times 10^4)$	58.565(19)	2
$\delta^{45} (\times 10^{10})$	-1184(22)	3	$\rho_{45} (\times 10^8)$	-52.79(90)	2
$\delta^{55} (\times 10^{10})$	-446(17)	3	$q_{04} (\times 10^3)$	-157.3485(36)	1.5
B_1	34.8877668(57)	0.991972(1)	$q_{05} (\times 10^3)$	-139.7165(36)	1.5
$D_1 (\times 10^6)$	47.8852(39)	2.0061(2)	$q_{44} (\times 10^5)$	53.45(33)	2
B_2	35.002840(20)	0.993256(1)	$q_{45} (\times 10^5)$	-237.3(13)	2
$D_2 (\times 10^6)$	48.107(60)	2.0277(36)	$q_{54} (\times 10^5)$	-330.1(14)	2
v_1	196576.8494(18)	0.47159(9)	$q_{55} (\times 10^5)$	-113.86(36)	2
v_2	198922.7020(21)	0.48114(7)	$q_{J4} (\times 10^8)$	117.82(19)	2.5
x_{11}	-743.8(66)	1	$q_{J5} (\times 10^8)$	115.351(69)	2.5
x_{12}	-350.2(39)	1	W	193.87198(96)	1
x_{13}	-3223(16)	1	$W_J (\times 10^5)$	-101.93(60)	2